Solvent-resolved fluorescent Ag nanocrystals capped with a novel terpyridine-based dye†

Yuanhao Gao,[a] Jieying Wu,[a] Qiong Zhao,[a] Lingxia Zheng,[a] Hongping Zhou,[a] Shengyi Zhang,[a] Jiaxiang Yang[a] and Yupeng Tian*[abc]

Received (in Durham, UK) 1st September 2008, Accepted 7th November 2008
First published as an Advance Article on the web 14th January 2009
DOI: 10.1039/b815115f

By using a novel terpyridine-based dye as a surface stabilizing agent, novel dye-capped Ag nanocrystals (NCs) were obtained. The growth dynamics of these dye-capped Ag NCs were monitored by UV-vis absorption spectroscopy. Interactions between the dye and the Ag NCs were investigated by ^{1}H NMR spectroscopy. The dye-capped Ag NCs showed solvent-resolved fluorescence in organic solvents, with full width at half-maximums (FWHM) as wide as ~100 nm, demonstrating the effect of the Ag NCs on the enhanced fluorescence of the capping dye.

Introduction

Metallic nanocrystals (NCs) have been of considerable interest in recent years due to their significant promise in the areas of optoelectronics, catalysis and biomedical applications.[1–5] The simplest and the most efficient synthetic method for metallic NCs is the reduction of metal cations. To ensure their stability, preparations require a stabilizing surface agent to control the rate of growth and prevent aggregation. Thiols, amines, carboxylic acids and even dendrimers are all quite useful to bind, stabilize and direct the growth of metal NCs. It has long been known that larger metal NCs (>5 nm) present strong surface plasmon absorption characteristics with essentially no fluorescence.[6,7] However, the fluorescence spectroscopy of dyes can be enhanced when the dye is attached to the surface of metal NCs.[8–10] This phenomenon, defined as metal-enhanced fluorescence (MEF), can be used to develop next-generation biological and chemical sensors.[11–13] An electromagnetic field is believed to exist near the metal core and cause MEF through coupling with the fluorophore.[14,15] Silver is the most common metal used for MEF due to its strong plasmon resonances and low absorption loss in the visible region.[13] However, the selection of appropriate dyes as surface agents, having optimum binding strength and steric bulkiness, is critical for the synthesis of dye-capped Ag NCs. Thiols and carboxylic acids have proved to be very efficient for the surface modification of Ag NCs due to their high affinity for Ag^+ ions. To date, much progress has been made in the optimization of thiol- and carboxylic acid-based dyes for MEF.[9,10] However, few examples describe the interaction between highly π-conjugated terpyridine-based dyes and Ag NCs. Here, we describe a simple and very efficient method leading to solvent-resolved fluorescent Ag NCs that relies on a novel terpyridine derivative as a surface stabilizing agent. The ligand is a large, highly π-conjugated system with terpyridine tridentate chelate groups as binding sites and three polyether tails as organo-soluble groups (labelled **L**, see Scheme 1). Besides the strong coordination of the terpyridine groups to Ag^+ ions,[16] the three flexible polyether chains are likely to lead to a "cage effect" and thus provide additional affinity for Ag^+ ions.[17] Consequently, ligand **L** will be very efficient for the immobilization of Ag^+ ions, serving as an Ag source for further reduction reactions. In the current experiments, the dye ligands, **L**, graft to the surface of Ag NCs and then interrupt their subsequent growth. Thus, it is easy to obtain target products of expected luminescence characteristics. The **L**-capped Ag NCs show solvent-resolved fluorescence with full width at half-maximums (FWHM) as wide as ~100 nm, demonstrating the effect of Ag NCs on the enhanced fluorescence of the capping ligand **L**. The interface structure of **L**-capped Ag NCs is investigated by ^{1}H NMR spectroscopy.

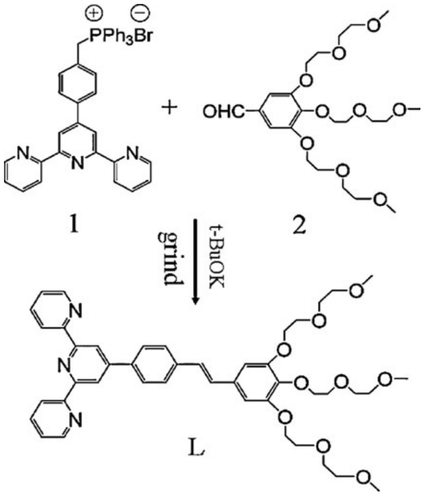

Scheme 1 The synthesis of ligand **L**.

---

[a] *Department of Chemistry, Anhui University, Hefei, 230039, PR China. E-mail: yptian@ahu.edu.cn. E-mail: gyh-1968@sohu.com; Fax: +86 551 5107342; Tel: +86 551 5108151*
[b] *State Key Laboratory of Coordination Chemistry, Nanjing University, Nanjing, 210093, PR China*
[c] *State Key Laboratory of Crystal Materials, Shandong University, Jinan, 250100, PR China*

† Electronic supplementary information (ESI) available: XRD pattern (Fig. S1), TGA diagram (Fig. S2), XPS spectra (Fig. S3) and time-resolved decay curves (Fig. S4 and Fig. S5). See DOI: 10.1039/b815115f

Experimental

All chemicals were available commercially, and the solvents were purified by conventional methods before use.

The synthesis and characterization of dye L

Dye **L** was synthesized by a solvent-free Wittig reaction[18] between 4-(2,2′:6′,2″-terpyridyl-4′)-benzyl triphenyl phosphonium bromide (**1**) and 3,4,5-tris-(2-(2-methoxyethoxy)ethoxy)-benzaldehyde (**2**), as shown in Scheme 1. Compound **1** was synthesized as described previously.[19] Compound **2** was prepared in an analogous way to that described in the literature.[20,21] For the synthesis of ligand **L**, **1** (2.0 g, 3.0 mmol), **2** (1.5 g, 3.1 mmol) and *t*-BuOK (1.3 g, 12.3 mmol) were placed into a dry mortar, milled vigorously for about 20 min and monitored by TLC until reaction completion. The mixture was dispersed in dichloromethane (200 mL). The organic phase was separated, washed with water (3×150 mL) and dried with Na_2SO_4. The solvent was removed and the residue was purified by column chromatography (alumina; 1% ethanol in petroleum ether) to yield pure compound **L** as colorless powder. Yield: 75%. ES-MS, *m*/*z* (%): 766.36 ($[M + H]^+$). ^1H NMR (acetone-d_6, 400 MHz, δ/ppm): 8.79 (s, 2H), 8.75 (d, 2H), 8.70 (d, 2H), 7.96 (t, $J = 7.8$ Hz, 2H), 7.87 (d, $J = 8.0$ Hz, 2H), 7.70 (d, $J = 8.0$ Hz, 2H), 7.45 (t, $J = 6.8$ Hz, 2H), 7.2 (s, 2H), 6.93 (s, 2H), 4.22–4.16 (m, 6H), 3.86–3.78 (m, 6H), 3.70 (t, 6H), 3.53 (t, 6H) and 3.32 (s, 9H). ^{13}C NMR (acetone-d_6, 100.61 MHz, δ/ppm): 205.63, 156.04, 155.80, 152.92, 149.24, 138.67, 138.42, 137.00, 136.87, 132.76, 129.69, 127.22, 127.16, 127.00, 124.14, 121.00, 117.92, 106.17, 71.86, 70.41, 69.60, 68.84 and 58.04.

Synthesis of L-capped Ag NCs

L-capped Ag NCs were synthesized by the reduction of $AgPF_6$ with $NaBH_4$ in an ethanol solution using **L** as a stabilizing agent. In the present experiment, dye **L** was utilized to immobilize Ag^+ ions, and subsequently to stabilize and solubilize Ag NCs in various organic solvents. Dye **L** (0.1523 g, 0.2 mmol) was firstly dissolved in ethanol (100 mL). Then, $AgPF_6$ (0.1265 g, 0.5 mmol) dispersed in ethanol (50 mL) was added dropwise to the above solution with magnetic stirring at room temperature for 30 min. At this stage, Ag^+ ions were immobilized *via* ligand **L** to form translucent **L**–Ag^+ sol, and the solution color gradually changed from colorless to pale yellow. Subsequently, a freshly prepared ethanol solution of 12 mL $NaBH_4$ (0.01 M) was injected into the pale yellow sol, instantly generating a gray-ish turbid solution, indicating the reduction of the Ag^+ ions. Stirring was continued for an additional 60 min, the color of the solution slowly turning to light pink, indicating the formation of high quality **L**-capped Ag NCs. To monitor the growth dynamics of the Ag NCs, aliquots were taken from the reaction mixture during their synthesis. The **L**-capped Ag NCs were precipitated by adding excess distilled water. Their powdery form was obtained by subsequent centrifugation of the precipitate, followed by washing it several times with a distilled water–ethanol mixture. The **L**-capped Ag NCs could easily redisperse in general organic solvents such as ethanol, dichloromethane, chloroform and DMF. For the optical characterization, the powder was redispersed in various organic solvents.

Characterization methods

Electrospray mass spectra (ES-MS) were obtained using a API400 mass spectrometer. ^1H NMR spectra of acetone-d_6 solutions (with TMS as an internal standard) were obtained using a Bruker Avance 400 MHz spectrometer. Ultraviolet-visible (UV-vis) absorption spectra were obtained using a Shimadzu UV-3600 UV-Vis-NIR spectrophotometer. Photoluminescence (PL) spectra were collected at room temperature using a Hitachi F-4500 fluorescence spectrophotometer. Time-resolved decay curves were obtained by a PicoQuant FluoTime 200 spectrometer, and the data were analyzed by a literature method.[22] TEM measurements were made using a Jeol JEM 2011 high resolution transmission electron microscope operating at 300 kV. X-Ray power diffraction (XRD) measurements were made using a Japan Rigaku DMax-γA rotation anode X-ray diffractometer operating with graphite-monochromatized Cu-K_α radiation ($\lambda = 1.54178$ Å). Thermogravimetric analyses (TGA) were performed under nitrogen at a heating rate of 10 °C min^{-1} using a Perkin-Elmer Pyris1 thermal analyzer. X-Ray photoelectron spectroscopy (XPS) data were recorded using a VG MK II spectrometer with a Mg-K_α source (1253.6 eV).

Results and discussion

The synthesis and characterization of L-capped Ag NCs

In this procedure, dye ligand **L** was used as a stabilizing agent to control the nucleation of Ag, and then to bind the Ag NCs. Due to the high affinity of **L** for Ag^+ ions, the pale yellow **L**–Ag^+ sol could form at room temperature. Fig. 1a and b show the absorption spectra of the free **L** solution and the **L**–Ag^+ sol, respectively. Initially, only free **L** contributes to the spectrum, with two characteristic absorption peaks at 283 and 340 nm (Fig. 1a). After the formation of the **L**–Ag^+ sol,

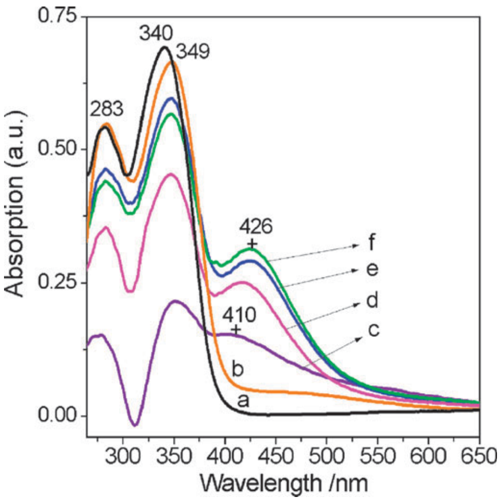

Fig. 1 UV-vis absorption spectra: (a) Free **L** solution and (b) **L**–Ag^+ sol. (c–f) The reaction mixture after reduction for (c) 3 min, (d) 10 min, (e) 30 min and (f) 60 min. The samples were diluted 10 times (v/v) in ethanol.

the **L** absorption peak of 340 nm is red-shifted to 349 nm, with an additional weak absorption band range in the range 400–600 nm (Fig. 1b), indicating strong coordination of **L** to the Ag^+ ions. Nucleation of the Ag occurs, forming small NCs when the $NaBH_4$ is injected into the pale yellow sol. The reduction reaction of the Ag^+ ions with $NaBH_4$ occurs so effectively that nucleation and growth of Ag NCs could be achieved within 30 min. The growth dynamics of the Ag NCs was monitored by absorption changes of the reaction mixture at different times. Fig. 1c–f show absorption spectra of the reaction mixture following the addition of $NaBH_4$ at different times. After 3 min, an absorption peak at 410 nm for the Ag particles appears, and further reduction leads to its increased intensity and a red-shifting. However, no obvious peak shift was observed for reduction times over 30 min, such as 60 min, which clearly demonstrates the suppression of the Ostwald ripening process (“defocusing”). The suppression of “defocusing” means that ligand **L** as a stabilizing agent has optimum binding strength and an appropriate steric bulkiness for the synthesis of stable Ag NCs. It is worth noting that no shifts of the absorption peaks of ligand **L** were observed during the reduction process with $NaBH_4$, which indicates that **L** is unable to react with $NaBH_4$ in this reduction process. However, the absorption intensities of ligand **L** increased with the growth of the Ag NCs. This could possibly arise from the influence of strong plasmon resonances of small Ag particles, which are dependant on their size.[6,7]

TEM images of the **L**-capped Ag NCs after a reaction time of 60 min showed nearly spherical particles, with particle sizes of 8–14 nm (Fig. 2). The XRD results revealed that these NCs are face-centered cubic Ag crystals (see ESI, Fig. S1†). The amount of **L** in the products was determined to be about 16 wt% by TGA measurements (see ESI, Fig. S2†). X-Ray photoelectron spectra (XPS) in the N 1s region revealed electronic interactions between the capping **L** and the Ag NCs (see ESI, Fig. S3†). Note, that the concentration of **L** in the synthetic system doesn’t appreciably change the particle size and size distribution of the Ag NCs. Upon further increasing the **L** content, the particle size, size distribution and **L** content on the surface of the Ag NCs don’t obviously change. One possibility could be due to the large difference between the rate of NC growth in the “focusing” regime and the rate of the Ostwald ripening process (“defocusing”). Also noteworthy is the aggregation effect of the **L**-capped Ag NCs in the solid state structure. The observed agglomeration of the **L**-capped Ag NCs in the TEM images could arise from the influence of capping **L** intermolecular $\pi\cdots\pi$, C–H$\cdots\pi$ or hydrogen bonding interactions. Highly π-conjugated ligands often take part in prolific intermolecular interactions to manipulate hybrid particles into an aggregate structure.[23]

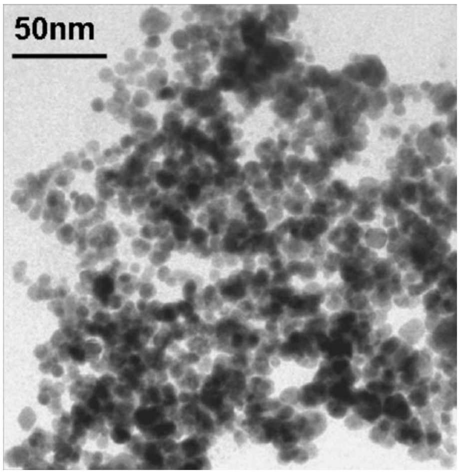

Fig. 2 TEM images of as-prepared **L**-capped Ag NCs.

^{1}H NMR spectroscopy is a credible measure for investigating the interface structure of organic–inorganic hybrid systems,[24] Fig. 3 showing our results. Fig. 3(a) shows the differences between the ^{1}H NMR spectrum of the aromatic/alkene moieties (terpyridinyl, benzyl, vinyl) of pure **L** and capping **L**, while Fig. 3(b) shows the changes to the polyether chain moieties of **L**. As shown in Fig. 3, the characteristic peaks of pure **L** are present in the spectrum of the **L**-capped Ag NCs, and integration shows that their ratio is the same as that in the spectrum of pure **L**. The main differences are the obvious peak shifts in the aromatic/alkene moieties and the obvious peak splitting in the polyether chain moieties. This is particularly evident in the aromatic region, where both proton peaks C2 (C2′) and C5 (C5′) of the terpyridinyl group shift upfield, while the other signals in the aromatic/alkene region shift downfield, yet integration gives the same number of protons as in pure **L**. The upfield shifts of both the C2 (C2′) and C5 (C5′) protons indicates that the conformational state of the terpyridine group has been altered into a tridentate chelate structure due to its coordination to Ag NCs, as shown in Fig. 3(a). The other aromatic moieties are close to the attachment point, which should cause a significant loss to their rotational mobilities and downfield shifts of their ^{1}H NMR chemical shifts. These observations confirm that all **L** ligands are covalently attached to the Ag NCs by the terpyridine group and that there is essentially no free **L**. Moreover, the observed proton resonances in the polyether chain moieties are not significantly shifted relative to free **L** in solution, but instead are all sharp, split signals, especially the terminal CH_3 group (C23) and adjacent CH_2 groups (C22, C21). This is an effect that is attributed to close packing of the polyether chains on the surface of the NCs, suggesting that the polyether chains are not the predominant binding sites *vs.* the tridentate terpyridine chelate group.

Photoluminescent properties of L-capped Ag NCs

The **L**-capped Ag NCs exhibited bright PL. As expected, a broad emission band centered at 506 nm with FWHMs as wide as ~100 nm was observed in the PL spectrum of **L**-capped Ag NCs (Fig. 4a). The broad emission band is believed to originate from the surface-capping **L** groups, since $NaBH_4$ reduction yields larger Ag NCs (8–14 nm) with essentially no fluorescence. However, the FWHM of 100 nm in the PL spectrum was much wider than that in the free **L** solution and the **L**–Ag^+ sol (Fig. 4b and c). The result demonstrates the effect of Ag NCs on the enhanced fluorescence of the capping **L**. Again, the emission peak position was considerably red-shifted relative to that of the free **L** solution and the **L**–Ag^+ sol. This could possibly arise from interactions

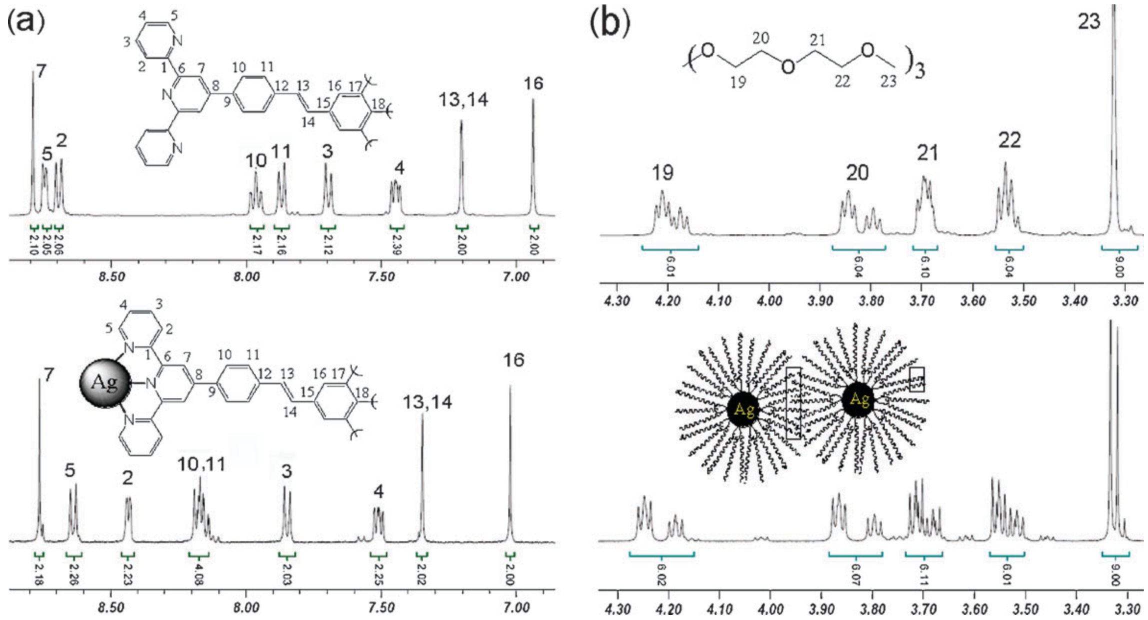

Fig. 3 Relevant peaks in the ^{1}H NMR spectra of pure **L** and **L**-capped Ag NCs in acetone-d_6: (a) The aromatic/alkene moieties of the pure **L** (upper) and **L**-capped (lower) Ag NCs. (b) The polyether chain moieties of the pure **L** (upper) and **L**-capped (lower) Ag NCs.

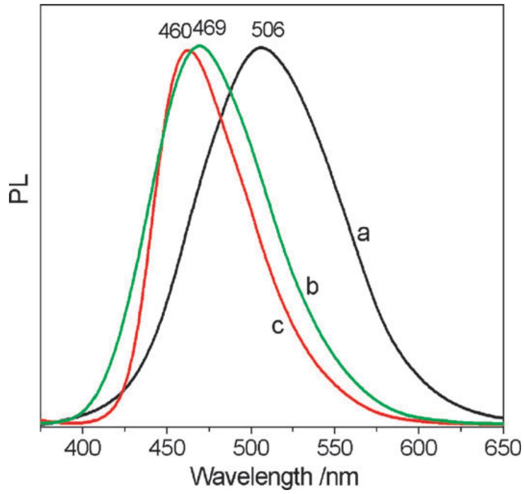

Fig. 4 PL spectra with excitation at 349 nm: (a) The as-prepared **L**-capped Ag NCs redispersed in ethanol, (b) the **L**–Ag$^+$ sol and (c) the free **L** ethanol solution.

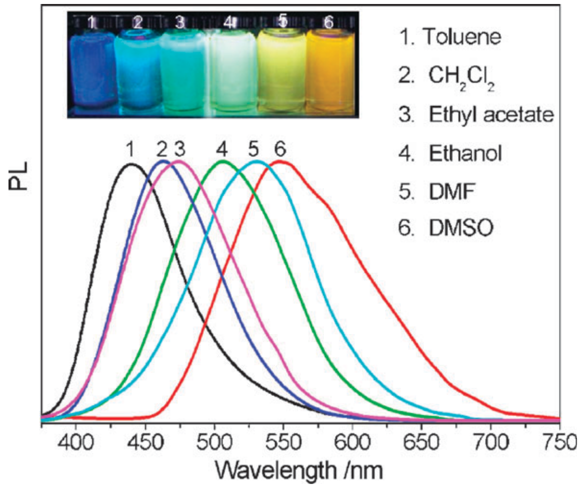

Fig. 5 The PL spectrum of **L**-capped Ag NCs in several solvents of differing polarity.

between the capping **L**'s ligand field and the electromagnetic field of the Ag core.

Significantly, the **L**-capped Ag NCs could easily redisperse in common organic solvents and exhibit a strong solvent-resolved fluorescence. Fig. 5 shows their emission spectrum in six common solvents of differing polarity. All spectra exhibited a broad emission band, and increasing the solvent's polarity gave rise to a red shift of the emission maximum. The red shift tendency is in agreement with that of pure **L**. Generally, the capping **L**'s molecular polarity and π-conjugated characteristics were responsible for the solvent-resolved PL. Importantly, the solutions were particularly stable and did not show any signs of precipitation or decomposition for more than 2 months. Also noteworthy were the fluorescence lifetimes. The fluorescence lifetime of the **L**–Ag NC hybrid system was τ = 1.503 ns in ethanol, which is obvious shorter than that (2.285 ns) of pure **L** (see ESI, Fig. S4 and Fig. S5†). Modification of the fluorescence lifetime was due to the interaction between the capping **L** and the Ag core. The emission of fluorophores capped on an Ag core is dependent on at least two factors: an enhanced local field and an increase in the intrinsic decay rate of the fluorophore, both due to MEF. The first factor provides stronger excitation rates but does not modify the fluorescence lifetime of the molecule. The second factor changes the quantum yield and lifetime of the fluorophore.[10,25] Unfortunately, the broad size distribution of the **L**-capped Ag NCs did not allow us to calculate the number of **L** ligands on the surface of the Ag particles, and so further elucidate the luminescence quantum efficiencies (QE).

Conclusions

In this work, a new, stable, fluorescent Ag system was prepared by capping **L** onto the surface of Ag NCs. ^{1}H NMR experiments indicated that the binding site of **L** was the terpyridine group, with covalent bonds to the Ag surface. Ligand **L** renders the Ag NCs soluble, with solvent-resolved fluorescence taking place in organic solvents. Due to MEF, the **L**-capped Ag NCs exhibit broad FWHMs, with a decrease in the average fluorescence lifetime. These features are expected to bring more opportunities of using **L**-capped Ag NCs for display, and biological and chemical sensors. Because of the high affinity of both the terpyridinyl group and polyether chains for metal salts, **L** could potentially be used for the fabrication of other metallic NCs with novel photoelectric properties.

Acknowledgements

This work was supported by the National Natural Science Foundation of China (50532030, 20771001 and 20871001), the Doctoral Program Foundation of the Ministry of Education of China (20050357001) and the Scientific Innovation Team Foundation of Anhui Province (2006KJ007TD).

References

1 J. D. Gibson, B. P. Khanal and E. R. Zubarev, *J. Am. Chem. Soc.*, 2007, **129**, 11653.
2 E. R. Zubarev, J. Xu, A. Sayyad and J. D. Gibson, *J. Am. Chem. Soc.*, 2006, **128**, 4958.
3 F. Porta, Z. Krpetić, L. Prati, A. Gaiassi and G. Scarić, *Langmuir*, 2008, **24**, 7061.
4 (*a*) C. W. Wang and M. G. Moffitt, *Chem. Mater.*, 2005, **17**, 3871; (*b*) Q. Dai, J. G. Worden, J. Trullinger and Q. Huo, *J. Am. Chem. Soc.*, 2005, **127**, 8008.
5 (*a*) B. K. Kuila, A. Garai and A. K. Nandi, *Chem. Mater.*, 2007, **19**, 5443; (*b*) C. Jiang, D. J. Cardin and S. C. Tsang, *Chem. Mater.*, 2008, **20**, 14.
6 (*a*) G. N. R. Tripathi and M. Clements, *J. Phys. Chem. B*, 2003, **107**, 11125; (*b*) A. Parfenov, I. Gryczynski, J. Malicka, C. D. Geddes and J. R. Lakowicz, *J. Phys. Chem. B*, 2003, **107**, 8829; (*c*) J. M. Nam, S. J. Park and C. A. Mirkin, *J. Am. Chem. Soc.*, 2002, **124**, 3820.
7 C. D. Geddes, H. Cao, I. Gryczynski, Z. Gryczynski, J. Y. Fang and J. R. Lakowicz, *J. Phys. Chem. A*, 2003, **107**, 3443.
8 (*a*) I. Gryczynski, J. Malicka, Y. B. Shen, Z. Gryczynski and J. R. Lakowicz, *J. Phys. Chem. B*, 2002, **106**, 2191; (*b*) J. Malicka, I. Gryczynski, Z. Gryczynski and J. R. Lakowicz, *Anal. Biochem.*, 2003, **315**, 57; (*c*) J. Malicka, I. Gryczynski, J. Fang, J. Kusba and J. R. Lakowicz, *Anal. Biochem.*, 2003, **315**, 160.
9 (*a*) J. Zhang and J. R. Lakowicz, *J. Phys. Chem. B*, 2005, **109**, 8701; (*b*) J. Zhang, J. Malicka, I. Gryczynski and J. R. Lakowicz, *J. Phys. Chem. B*, 2005, **109**, 7643; (*c*) F. Xie, M. S. Baker and E. M. Goldys, *J. Phys. Chem. B*, 2006, **110**, 23085.
10 K. Ray, R. Badugu and J. R. Lakowicz, *J. Am. Chem. Soc.*, 2006, **128**, 8998.
11 (*a*) P. J. G. Goulet, N. P. W. Pieczonka and R. F. Aroca, *Anal. Chem.*, 2003, **75**, 1918; (*b*) S. J. Lee and K. Kim, *Chem. Commun.*, 2003, **2**, 212; (*c*) S. P. Mulvaney, M. D. Musick, C. D. Keating and M. J. Natan, *Langmuir*, 2003, **19**, 4784.
12 T. A. Taton, R. C. Mucic, C. A. Mirkin and R. L. Letsinger, *J. Am. Chem. Soc.*, 2000, **122**, 6305.
13 S. L. Pan, Z. J. Wang and L. J. Rothberg, *J. Phys. Chem. B*, 2006, **110**, 17383.
14 (*a*) M. Kerker and C. G. Blatchford, *Phys. Rev. B: Condens. Matter Mater. Phys.*, 1982, **26**, 4082; (*b*) J. Zhang, J. K. Whitesell and M. A. Fox, *J. Phys. Chem. B*, 2003, **107**, 6051.
15 D. D. Evanoff, R. L. White and G. Chumanov, *J. Phys. Chem. B*, 2004, **108**, 1522.
16 (*a*) J. Hannon, C. L. Painting, E. A. Plummer, L. J. Childs and N. W. Alcock, *Chem.–Eur. J.*, 2002, **8**, 2225; (*b*) L. Hou and D. Li, *Inorg. Chem. Commun.*, 2005, **8**, 128.
17 (*a*) M. E. Fragala, G. Malandrino, O. Puglisi and C. Benelli, *Chem. Mater.*, 2000, **12**, 290; (*b*) J. P. Gao, J. Fu, C. K. Lin, J. Lin, Y. C. Han, X. Yu and C. Y. Pan, *Langmuir*, 2004, **20**, 9775.
18 J. X. Yang, X. T. Tao, C. X. Yuan, Y. X. Yan, L. Wang, Z. Liu, Y. Ren and M. H. Jiang, *J. Am. Chem. Soc.*, 2005, **127**, 3278.
19 Z. J. Hu, J. X. Yang, Y. P. Tian, X. T. Tao, L. Tian, H. P. Zhou, G. B. Xu, W. T. Yu, Y. X. Yan, Y. H. Sun, C. K. Wang, X. Q. Yu and M. H. Jiang, *Bull. Chem. Soc. Jpn.*, 2007, **80**, 986.
20 M. A. Oar, J. M. Serin, W. R. Dichtel, J. M. J. Frechet, T. Y. Ohulchanskyy and P. N. Prasad, *Chem. Mater.*, 2005, **17**, 2267.
21 V. Percec, M. Peterca, M. J. Sienkowska, M. A. Ilies, E. Aqad, J. Smidrkal and P. A. Heiney, *J. Am. Chem. Soc.*, 2006, **128**, 3324.
22 J. R. Lakowicz, *Principles of Fluorescence Spectroscopy*, Kluwer Academic/Plenum, New York, 2nd edn, 1999.
23 J. Jin, T. Iyoda, C. S. Cao, Y. L. Song, L. Jiang, T. J. Li and D. B. Zhu, *Angew. Chem., Int. Ed.*, 2001, **40**, 2135.
24 (*a*) F. Porta, Z. Krpetić, L. Prati, A. Gaiassi and G. Scarić, *Langmuir*, 2008, **24**, 7061; (*b*) C. Querner, P. Reiss, J. Bleuse and A. Pron, *J. Am. Chem. Soc.*, 2004, **126**, 11574; (*c*) C. Querner, A. Benedetto, R. Demadrille, P. Rannou and P. Reiss, *Chem. Mater.*, 2006, **18**, 4817.
25 (*a*) J. R. Lakowicz, *Anal. Biochem.*, 2005, **337**, 171; (*b*) J. R. Lakowicz, *Plasmonics*, 2006, **1**, 5; (*c*) J. Malicka, I. Gryczynski, J. Kusba and J. R. Lakowicz, *Biopolymers*, 2003, **70**, 595.